Author Manuscript

Author Manuscript

Author Manuscript

Author Manuscript

HHS Public Access

Author manuscript

Hepatology. Author manuscript; available in PMC 2016 May 01.

Published in final edited form as:

Hepatology. 2015 May ; 61(5): 1591–1602. doi:10.1002/hep.27665.

CXCR4 inhibition in tumor microenvironment facilitates anti-PD-1 immunotherapy in sorafenib-treated HCC in mice

Yunching Chen[1,2,#], **Rakesh R. Ramjiawan**[1,3,#], **Thomas Reiberger**[1,4,#], **Mei R. Ng**[1], **Tai Hato**[1], **Yuhui Huang**[1,¶], **Hiroki Ochiai**[1,§], **Shuji Kitahara**[1], **Elizabeth C. Unan**[1], **Tejaswini P. Reddy**[1], **Christopher Fan**[1], **Peigen Huang**[1], **Nabeel Bardeesy**[5], **Andrew X. Zhu**[5], **Rakesh K. Jain**[1], and **Dan G. Duda**[1,*]

Yunching Chen: yunching@mx.nthu.edu.tw; Rakesh R. Ramjiawan: rramjiawan@steele.mgh.harvard.edu; Thomas Reiberger: reiberger@steele.mgh.harvard.edu; Mei R. Ng: rosang@steele.mgh.harvard.edu; Tai Hato: thato@partners.org; Yuhui Huang: hyhui20126@163.com; Hiroki Ochiai: hochiai410@gmail.com; Shuji Kitahara: SKITAHARA@mgh.harvard.edu; Elizabeth C. Unan: unane@bc.edu; Tejaswini P. Reddy: treddy@wellesley.edu; Christopher Fan: christopher.fan@duke.edu; Peigen Huang: peigen@steele.mgh.harvard.edu; Nabeel Bardeesy: bardeesy.nabeel@mgh.harvard.edu; Andrew X. Zhu: azhu@partners.org; Rakesh K. Jain: jain@steele.mgh.harvard.edu; Dan G. Duda: duda@steele.mgh.harvard.edu

[1]E.L Steele Laboratory for Tumor Biology, Dept. of Radiation Oncology, Massachusetts General Hospital Cancer Center, Harvard Medical School, Boston, MA [2]Institute of Biomedical Engineering, National Tsing Hua University, Hsinchu, Taiwan [3]Angiogenesis Laboratory, Cancer Center Amsterdam, Department of Medical Oncology, VU University Medical Center, Amsterdam, The Netherlands [4]Division of Gastroenterology & Hepatology, Medical University of Vienna, Vienna, Austria [5]Department of Medicine, Cancer Center, Massachusetts General Hospital and Harvard Medical School, Boston, MA

Abstract

Sorafenib—a broad tyrosine kinase inhibitor—is the only approved systemic therapy for advanced hepatocellular carcinoma (HCC), but provides limited survival benefits. Recently, immunotherapy has emerged as a promising treatment strategy, but its role remains unclear in HCCs, which are associated with decreased cytotoxic CD8+ T-lymphocyte infiltration in both murine and human tumors. Moreover, we have shown in mouse models that after sorafenib treatment, intratumoral hypoxia is increased and may fuel evasive resistance. Using orthotopic HCC models, we now show that increased hypoxia after sorafenib treatment promotes immunosuppression, characterized by increased intratumoral expression of the immune checkpoint inhibitor programmed death-ligand 1 (PD-L1) and accumulation of T-regulatory cells and M2-type macrophages. We also show that the recruitment of the immunosuppressive cells is mediated in part by hypoxia-induced upregulation of stromal cell-derived 1 alpha (SDF1α). Inhibition of the SDF1α receptor (C-X-C receptor type 4 or CXCR4) using AMD3100 prevented the polarization toward an immunosuppressive microenvironment after sorafenib treatment, inhibited tumor growth, reduced lung metastasis, and improved survival. However, combination of AMD3100 and sorafenib did

[*]Corresponding author: Dan G. Duda, DMD, PhD, Steele Laboratory for Tumor Biology, Massachusetts General Hospital, Cox-734, 100 Blossom Street, Boston, MA 02114; phone: (617) 726-4648; fax: (617) 726-1962; duda@steele.mgh.harvard.edu.
[#]These authors contributed equally to this work.
[¶]Cyrus Tang Hematology Center at Soochow University, China
[§]National Cancer Institute, Tokyo, Japan.

Author Manuscript Author Manuscript Author Manuscript Author Manuscript

not significantly change cytotoxic CD8+ T-lymphocyte infiltration into HCC tumors and did not modify their activation status. In separate experiments, antibody blockade of the PD-L1 receptor PD-1 showed anti-tumor effects in treatment-naïve tumors in orthotopic (grafted and genetically engineered) models of HCC. However, anti-PD-1 antibody treatment had additional anti-tumor activity only when combined with sorafenib and AMD3100, and not when combined with sorafenib alone.

Conclusion—Anti-PD-1 treatment can boost anti-tumor immune responses in HCC models. When used in combination with sorafenib, this immunotherapy approach shows efficacy only with concomitant targeting of the hypoxic and immunosuppressive microenvironment with agents such as CXCR4 inhibitors.

Keywords

Immunosuppression; hypoxia; immune checkpoint; T lymphocytes; tumor-associated macrophages

INTRODUCTION

Sorafenib is a multi-targeted TKI and a worldwide standard of care for advanced HCC patients based on increased survival data from two phase III trials (1, 2). However, these studies also showed that HCCs rapidly become sorafenib-resistant, with a short time to progression. Due to promiscuous target inhibition by sorafenib, the mechanisms of treatment evasion are likely multifactorial. One mechanism may be the increase in tissue hypoxia after prolonged antiangiogenic therapy, which likely promotes tumor recurrence locally and at distant sites (3–5). Hypoxia can fuel resistance to treatment not only by promoting genomic instability, angiogenesis and invasion, but also by creating an immunosuppressive microenvironment (4, 6–10). Increased hypoxia results in recruitment and activation of multiple myeloid and lymphoid immune suppressor cells such as M2-type TAMs, myeloid-derived suppressor cells, and Tregs (10, 11). Indeed, we have previously found that alleviating hypoxia in breast cancers enhanced the efficacy of a vaccine therapy (12). In HCC, we demonstrated that increased hypoxia after sorafenib treatment induced SDF1α and CXCR4 expression and Gr-1+ myeloid-derived suppressor cell recruitment (13). Blockade of SDF1α/CXCR4 axis prevented the increase in tumor desmoplasia and inhibited tumor growth despite persistent hypoxia (13).

Discovery of the mechanistic link between hypoxia, inflammation, fibrosis and HCC progression involving SDF1α/CXCR4 pathway prompted us to test whether sorafenib also modulates the immune microenvironment in HCC via this pathway. Clinical data regarding the presence, infiltration and function of TILs in HCC are limited. Case reports and a cohort study report the rare presence of TILs in human HCCs (14–16). Moreover, TIL presence and function may be a prognostic marker in HCC patients (17). Therefore, a combination of depletion of Treg cells and concomitant stimulation of effector T cells may represent an effective strategy to reduce HCC metastasis and recurrence (18, 19). T cell activation using antibody blockade of the immune checkpoint PD-1 has been successfully used for treatment of late stage melanoma, and an anti-PD-1 antibody (pembrolizumab) was recently granted accelerated approval by the US FDA. Anti-PD-1 antibodies have also shown efficacy in

Author Manuscript Author Manuscript Author Manuscript Author Manuscript

other solid tumors (20). But achieving similar efficacy with immune checkpoint inhibitors in HCC will largely depend on how it is integrated with sorafenib. For example, it has also been recently shown that cancer cells, cancer-associated stromal cells and a hypoxic tumor microenvironment can upregulate immune regulatory proteins—immune checkpoint inhibitors such as PD-L1 or its receptor PD-1—that facilitate tumor escape from immune surveillance (21, 22). Upregulation of PD-L1/PD-1 inhibits cytotoxic CD8+ T-lymphocyte activation and proliferation and further contributes to resistance and progression of solid tumors. However, until now experimental data on the direct effects of sorafenib on cancer cells and the immune microenvironment in HCCs are lacking. Here, we used orthotopic (grafted and genetically engineered) murine models of HCC to examine the role of targeting CXCR4 pathway in the absence or presence of PD-1 blockade on primary tumor growth, lung metastasis, and the immune microenvironment after sorafenib treatment.

EXPERIMENTAL PROCEDURES

Cells

We used the murine HCC cell line HCA-1 (13), and human HCC cell lines JHH-7 and Hep3B (ATCC) (Suppl. Material).

HCC models

Orthotopic implantation was performed as described (13) (Suppl. Material). We also induced hepatocarcinogenesis and liver fibrosis in *Mst1*$^{-/-}$*Mst2*$^{F/-}$ mice, as described (13, 23) (Suppl. Material).

Imaging

The growth of intrahepatic HCCs was evaluated by high-frequency ultrasound imaging (VisualSonics, Toronto, Canada) by operators blinded to the treatment (Suppl. Material, Fig. S1). The presence of abdominal metastasis was defined as extra-hepatic tumor mass infiltrating neighboring organs, significant lymph node enlargement, or peritoneal carcinomatosis. Presence and number of lung metastases were recorded for the different treatment groups as assessed macro- and microscopically in both lungs after sacrificing the animals.

Treatment

The maximal tumor diameters were measured in two dimensions to calculate tumor volume by the formula (a/2*b/2*b/2)*4/3*Pi. Tumor dimensions were either measured by calipers at the experimental endpoint (after 2 weeks of treatment) or by ultrasound starting 1 week after implantation, where tumor size was typically 3×3mm (corresponding to a tumor volume of ~14mm^3). At that time, the mice were randomized according to tumor size to the treatment groups to ensure similar tumor sizes at baseline (pretreatment) when treatment was started. Treatment included daily gavage with PBS/vehicle (control group) or sorafenib at a dose of 50mg/kg (in PBS/1%Tween80, MGH Pharmacy), and with the CXCR4 inhibitor AMD3100 (10mg/kg bodyweight, s.c. by osmotic minipumps, Sigma). In separate experiments, these treatments were combined with antibody against murine PD-1 (100μg i.p. every 3 days, for a total of 5 times).

Author Manuscript Author Manuscript Author Manuscript Author Manuscript

Cell viability assays

Cell viability was assessed using the nucleic acid stain SYTO 60 (Invitrogen). Cells (3,000 per well) were seeded into 96-well plates, allowed to adhere overnight, and exposed to a range of drug concentrations. After 72hr, cells were fixed in 4% formaldehyde, stained with SYTO-60, and cell viability was assessed by fluorescence measurement using a SpectraMax M5 microplate reader (excitation 630nm, emission 695nm; Molecular Devices). The fraction of control was calculated by dividing the fluorescence obtained from the drug-treated cells by the fluorescence obtained from the control (no drug)-treated cells.

Assessment of Apoptosis by TUNEL Staining and Cleaved-Caspase 3 Staining

Frozen sections of HCC tissues were stained by using TACS™ TdT Kit (R&D Systems, Minneapolis, MN) according to manufacturer's protocol. The apoptotic cells were counted in four randomly selected visual fields for each sample. The apoptotic index was calculated as the fraction of apoptotic nuclei.

Immunohistochemistry and immunofluorescence

For evaluation of vascular density, frozen tumor sections (7–8μm thick) were immunostained with primary antibodies against CD31 (for endothelial cells) and counterstained with fluorescent secondary antibodies. Samples were imaged by using an Olympus confocal microscope and quantified using 4–5 random fields per sample. Pimonidazole (Hypoxyprobe, Hypoxyprobe Inc.) was used as a marker of hypoxia. Hypoxyprobe (60mg/kg bodyweight) was injected i.p. 30min before the animals were sacrificed. Tumors were harvested and processed immediately. Hypoxia was assessed in frozen tissue sections by IF staining of pimonidazol by anti-Hypoxyprobe-FITC-labeled antibody.

To evaluate the number and distribution of CD8+ T-lymphocytes, frozen sections of HCC samples were stained for CD8+ positive cells and nuclear staining with DAPI. Whole tumor sections were scanned using mosaic confocal microscopy. The number of CD8+ T lymphocytes was recorded both in tumor margin (200μm) and in tumor center (3 tumor samples per groups were assessed, 6 random regions were selected both for tumor margin and for tumor center; 4 groups x 3 mice x 6 peripheral x 6 central tumor regions). In addition, we performed immunostaining for CD8 and PD-L1/CD274 in human HCC samples (n=16), obtained under an approved IRB protocol. We evaluated the number and distribution of intratumoral CD8+ T-lymphocytes (margin vs. center) in a similar manner.

Flow Cytometry

Tumor tissues were harvested and prepared for flow cytometry as previously described (12) (Suppl. Material). Flow cytometric data were obtained using a LSR-II flow cytometer (Becton Dickinson) and analyzed with FACSDiva™ software. We used the following monoclonal anti-mouse antibodies: CD4-FITC, CD4-PE-Cy7, CD8a-FITC, CD8a-PE, CD45-PE, CD45-PE-Cy7, CD25-APC-Cy7, FoxP3-APC, Gr-1-APC and CD11b-APC-Cy7 (BD Biosciences) and F4/80-FITC, F4/80-PE (eBioscience) (see Suppl. Fig. S2).

Author Manuscript Author Manuscript Author Manuscript Author Manuscript

Western Blotting

We used antibodies for PD-L1 (Abcam, Cambridge, MA) to measure the levels of this immune checkpoint in HCC tissues and HCA-1 cells (Suppl. Material).

Quantitative RT-PCR

Total RNA was extracted with RNeasy® Mini-Kit (Qiagen) from flow cytometry-sorted viable TAMs (7AAD–CD45+F4/80+Gr-1– cells). cDNAs were synthesized using TaqMan® RT Kit (Applied Biosystems, Brachburg, NJ). We used specific primers for β-actin, Arg-1, IL-1β, IL-10, IL-12, TNF-α, iNOS, CCL17, CCL22, CXCR4, CXCL10, MMP-9 and TGF-β, and determined the relative level of gene expression by using Real-Time SBYR Green PCR master mix (Applied Biosystems) on a Stratagene Mx3000P qPCR System, as described (12).

Protein measurements using multiplexed ELISA

Frozen tumors of each group were prepared using a lysis cocktail buffer (RIPA buffer, Boston Bioproducts Inc., Boston, MA) including phosSTOP, cOmplete (Roche, Indianapolis, IN). Tumors were homogenized with a tissue homogenizer (Qiagen, Valencia, CA), and the suspensions were sonicated using a sonicator (Branson, Notredam, IN). All samples were prepared at a protein concentration of 2μg/ml. The pro-inflammatory Panel 1 Mouse V-PLEX kit was used to measure the concentration of several cytokines – IL-1β, IL-2, IL-6, IL-8, IL-12, IFN-γ, TNF-α and KC-Gro (Meso Scale Discovery, Rockville, MD).

Statistical analysis

All statistical analyses were performed by Graph Pad prism. Student *t*-test or Mann-Whitney U test were used according to data distribution. Numbers of animals (proportions) with metastases were compared by Chi-Square test. A *p*-value of less than 0.05 was considered statistically significant.

RESULTS

CXCR4 inhibition during sorafenib treatment has anti-vascular and anti-metastatic effects and delays HCC progression

Blockade of SDF1α/CXCR4 axis by continuous infusion of AMD3100 using osmotic pumps significantly delayed the primary growth of orthotopic HCA-1 tumors in immunocompetent C3H mice when combined with daily sorafenib treatment as compared to either treatment alone (Fig. 1A). In the HCA-1 HCC model, mice develop spontaneous lung metastases that are detectable 28 days after intra-hepatic tumor implantation. Despite delaying the primary tumor growth, sorafenib did not affect metastasis formation or overall survival compared to control-treated mice (Fig. 1B,C). In contrast, the addition of AMD3100 treatment significantly inhibited lung metastasis, and led to an increase in overall survival (Fig. 1B,C). The tumor growth delay was seen after combination therapy was reproduced in orthotopic human HCC xenograft models using Hep3B and JHH-7 cells (Suppl. Fig. S3). Of interest, tumor growth inhibition occurred in the face of minor direct

Author Manuscript Author Manuscript Author Manuscript Author Manuscript

effects of recombinant SDF1α or AMD3100 on HCC or endothelial cell proliferation after sorafenib treatment *in vitro* (Suppl. Material, Fig. S4). However, sorafenib treatment significantly reduced intratumoral microvascular density (MVD) and increased hypoxia and SDF1α expression, and addition of AMD3100 to sorafenib enhanced the anti-vascular effects of treatment (Suppl. Fig. S5). Moreover, we found that CXCR4 inhibition prevented the increase in EMT markers in HCC cells cultured in hypoxic conditions, in a dose-dependent manner (Suppl. Material, Fig. S6). Thus, the inhibition of HCC progression induced by sorafenib and AMD3100 in these HCC models is at least in part due to tumor microenvironment-mediated effects.

CXCR4 inhibition prevents the polarization towards an immunosuppressive HCC microenvironment during sorafenib treatment

We next examined the effects of sorafenib treatment on tumor inflammatory cell infiltration by flow cytometric analyses of enzymatically digested HCC tissue. While the fraction of CD45+ immune cells of the total number of viable cells did not change significantly, we found that sorafenib increased the numbers of F4/80+ TAMs, and CD11b+Gr-1+ and CD45+CXCR4+ myeloid cells in both HCA-1 and JHH-7 HCC models (Fig. 2A–C, Suppl. Fig. S7). Moreover, sorafenib treatment resulted in an increase in the fraction of tumor-infiltrating CD4+CD25+FoxP3+ Tregs in HCA-1 tumors ($p<0.05$)(Fig. 2D). Addition of AMD3100 to sorafenib significantly decreased the fraction of F4/80+ TAMs, CD11b+Gr-1+ myeloid cells and CD4+CD25+FoxP3+ Tregs in the orthotopic HCA-1 model to levels comparable to those of treatment-naive (control) HCCs (Fig. 2).

Both VEGF and SDF1α have been reported to mediate the trafficking and retention of tumor-infiltrating myeloid (bone marrow-derived) cell populations (F4/80+ TAMs, Gr-1+ monocytic and granulocytic populations) in other tumor types and in the normal liver (24–28). However, it is currently unknown how inhibitors of these pathways affect bone marrow-derived cell activation and functional cytokine secretion. To examine this, we sorted F4/80+ TAMs using flow cytometry from digested HCC tissue after 14 days of treatment, extracted mRNA and performed qPCR analysis to measure widely accepted markers of angiogenesis and of M1– and M2-type of activation (8, 29). TAMs from sorafenib-treated HCCs expressed more than 2-fold higher levels of CXCR4 and VEGF as well as the M2-type markers CCL22 and Arg-1 compared to TAMs from control HCCs (Suppl. Table S1). On the other hand, the expression of the M1-type markers was not significantly altered in TAMs in sorafenib-treated HCCs (Suppl. Table S1). AMD3100 alone or in combination with sorafenib reduced the expression of M2-type markers in TAMs without affecting that of M1-type markers (Suppl. Table S1). To examine whether sorafenib and AMD3100 treatments also affect the infiltration and proliferation of T-lymphocytes in HCC, we further assessed the fraction of tumor-infiltrating $CD4^+$ and $CD8^+$ T-lymphocytes. Combination treatment of sorafenib and AMD3100 or sorafenib alone did not increase the fraction of $CD4^+$ and $CD8^+$ T-lymphocytes (Fig. 2E,F). Thus, blockade of SDF1α/CXCR4 axis may inhibit sorafenib-induced immunosuppression in the HCC but is insufficient to enhance T-lymphocyte infiltration.

Author Manuscript Author Manuscript Author Manuscript Author Manuscript

PD-L1 is expressed by HCC cells and is increased after sorafenib treatment

Hypoxia has been shown to upregulate the expression of immune regulatory proteins such as PD-1/PD-L1, which inhibit cytotoxic CD8+ T-lymphocyte proliferation and activation. We next evaluated if treatment-induced hypoxia increases PD-L1 expression in HCA-1 tumors. Immunocompetent mice bearing orthotopic HCA-1 tumors were treated when the tumor reached a size of 14mm^3. Tumors were treated with sorafenib for 28 days and then the mice were sacrificed and tumors were collected. Western blot analysis showed that sorafenib treatment resulted in increased PD-L1 expression in HCA-1 tumors compared with control treated tumors (Fig. 3A). We next examined the cell types that express PD-L1 in HCC. We found that cultured HCA-1 cells expressed detectable levels of PD-L1 (Suppl. Fig. S8A). By flow cytometry of digested tumor tissue, we detected, as expected, expression of PD-L1 on multiple hematopoietic cells, including on a fraction of Gr-1+ cells, TAMs, dendritic cells and lymphocytes (Suppl. Table S2). In addition, analysis of resected human HCC tissues showed PD-L1 expression in both cancer cells and immune cells infiltrating the tumor stroma (Suppl. Fig. S8B,C). Finally, immunofluorescence analysis of HCA-1 tumors showed co-localization of PD-L1 expression with pimonidazole staining of hypoxic tissue (Suppl. Fig. S8D). These data suggest that PD-L1 expression by the cancer cells and HCC stromal cells, particularly in hypoxic regions, may play a role in immunosuppression after sorafenib treatment.

PD-1 blockade combined with CXCR4 inhibition and sorafenib delays HCC growth

We next examined whether blocking the PD-1 improves the efficacy of sorafenib and CXCR4 inhibition during persistent hypoxia. To this end, we assessed the efficacy of anti-PD-1 treatment alone, or in combination with sorafenib plus/minus AMD3100 (Suppl. Fig. S9A). Average body weight was similar across all treatment groups, and no other signs of toxicity were observed. Wound healing (after median laparotomy) was not impaired in any of the treatment groups. As expected, the sorafenib/AMD3100 combination significantly inhibited HCA-1 tumor growth. Moreover, anti-PD-1 treatment alone showed comparable efficacy. Interestingly, combining sorafenib with anti-PD-1 treatment did not show efficacy, while the triple-combination group (sorafenib/AMD3100/anti-PD-1) showed the most pronounced delay in tumor growth versus the control group (Fig. 3B, Suppl. Fig. S10A). Furthermore, the number of lung metastases was significantly reduced by anti-PD-1 treatment alone and by sorafenib plus AMD3100, and it was further inhibited by addition of anti-PD-1 treatment (Fig. 3C). Neither sorafenib alone nor anti-PD-1 antibody with sorafenib affected spontaneous lung metastasis formation.

Next, we sought to further confirm the activity of anti-PD-1 therapy in a genetically engineered (*Mst*-mutant) model of HCC in mice with cirrhotic livers (13)(Suppl. Fig. S9B). Using US imaging in this model, we found that anti-PD-1 treatment may stabilize the growth of established HCCs. Moreover, we found that combination of anti-PD-1 antibody with sorafenib and AMD3100—but not anti-PD-1 antibody with sorafenib alone—led to regression of established tumors (Fig. 3D, Suppl. Fig. S10B).

Author Manuscript Author Manuscript Author Manuscript Author Manuscript

PD-1 blockade combined with CXCR4 inhibition and sorafenib increases tumor cell death in vivo

We next evaluated whether the efficacy see with addition of anti-PD-1 treatment to sorafenib plus AMD3100 is due to increased tumor cell death. We found tumors in the triple combination group had extensive areas of tumor necrosis in the HCA-1 tumors, which were not detectable to a similar extent in any of the other treatment groups (Fig. 4A). We next quantified cell apoptosis and found that the addition of anti-PD-1 to sorafenib and AMD3100 dramatically increased the number of cleaved caspase 3-positive cells in tumors compared to the other groups (Fig. 4B). Similar findings were obtained after analyzing HCC tissues from *Mst* mutant mice (Fig. 4C). Thus, adding anti-PD-1 antibody to sorafenib and AMD3100 treatment significantly decreases primary tumor growth by triggering tumor necrosis and apoptosis and further reduces the incidence of lung metastases.

Addition of anti-PD-1 treatment to sorafenib and AMD3100 increases intratumoral penetration and activation of CD8+ T-lymphocytes in HCC

We first examined the pattern of lymphocyte distribution in treatment-naïve human HCCs, and found significantly reduced numbers of CD8+ T-lymphocytes penetrating into tumor proper as compared to tumor margin (Suppl. Fig. S11). We next performed a similar analysis as well as flow cytometric analyses of lymphocytic populations in the murine HCCs. We also evaluated whether the effects of adding anti-PD-1 treatment increases or activates anti-tumor T-lymphocytes. We first assessed the percentages of CD8+ T-lymphocytes (cytotoxic T cells), in HCC tissues from mice in different treatment groups by flow cytometry. We found no difference in the fraction of these cells normalized either to the total number of CD45+ tumor-infiltrated leukocytes or to the total number of cells across treatment groups in HCA-1 tumor grafts or HCCs induced in *Mst* mutant mice (Suppl. Fig. S12). We then examined the distribution of the CD8+ T-lymphocytes in tumor sections by immunofluorescence staining. Sorafenib alone did not alter CD8+ T-lymphocyte number or distribution, and the combination of sorafenib and AMD3100 only slightly increased the number of CD8+ T-lymphocytes localized deeper within the primary tumors. Addition of anti-PD-1 treatment to sorafenib and AMD3100 significantly increased cell intratumoral penetration by CD8+ T-lymphocytes in both models (Fig. 5). The tumor-infiltrating CD8+ T-lymphocytes co-localized with apoptotic cells within the HCCs (Fig. 4B).

To test whether if these tumor-infiltrating CD8+ T-lymphocytes were activated after PD-1 blockade, we evaluated biomarkers of activation, i.e., IFN-γ, IL-2 and TNF-αexpression levels. ELISA analysis showed that addition of anti-PD-1 treatment to sorafenib and AMD3100 significantly increased the intratumoral levels of IFN-γ, IL-2 and TNF-α by 50–130% compared to control (Fig. 6). In contrast, sorafenib or anti-PD-1 alone and the combination treatment of sorafenib plus AMD3100 or sorafenib plus anti-PD-1 did not significantly change IFN-γ, IL-2 and TNF-α expression levels (Fig. 6). Similarly, only triple combination treatment significantly increased IFN-γ, IL-2 and TNF-α expression levels in genetically induced tumors in *Mst*-mutant mice (Suppl. Fig. S13).

Author Manuscript Author Manuscript Author Manuscript Author Manuscript

DISCUSSION

HCC is a highly vascularized tumor, and the anti-angiogenic agent sorafenib showed increased survival in two large phase III trials in HCC patients (1, 2). Unfortunately, recent experience with various other anti-angiogenic agents has shown that many HCC tumors are highly resistant to anti-angiogenic therapy (30, 31). Several recent reports converged to the conclusion that the increase in recruitment of myeloid-derived cell populations to tumors represents a critical step in emergence of resistance to anti-VEGF therapy and facilitates tumor progression [reviewed in (32)]. Indeed, we have previously shown in orthotopic (in both grafted and genetically engineered) models of HCC in mice that increased intratumoral hypoxia after sorafenib treatment led to increased SDF1α expression, which promoted treatment resistance. We now show that SDF1α/CXCR4 axis also promotes tumor vascularization, likely via recruitment of pro-angiogenic myeloid cells (33). In addition to pro-angiogenic and pro-inflammatory effects, hypoxia can trigger EMT in cancer cells, which may play an important role in tumor progression and particularly in metastasis (34). We show that SDF1α/CXCR4 pathway can directly mediate transition to an EMT phenotype in HCC cells in a hypoxic microenvironment. Collectively, these data may explain the unaltered progression of the disease at distant sites in the face of sorafenib treatment. Indeed, CXCR4 blockade prevented EMT despite persistence hypoxia, reduced metastatic burden, and increased survival in mice with HCC. These findings may be relevant not only for sorafenib but for any other hypoxia-inducing therapy in HCC.

We also found that—in addition to Gr-1+ myeloid cells—there is an increase in M2-type TAMs and Tregs in HCA-1 tumors after sorafenib treatment indicating the induction of an immunosuppressive microenvironment in sorafenib-treated HCCs. CXCR4 blockade reduced the infiltration of these immunosuppressive cells in these HCCs despite persistent hypoxia, but failed to promote anti-tumor cellular immune responses. Here we provide proof-of-the-principle data that addition of the immune checkpoint inhibitor anti-PD-1 antibody to AMD3100 and sorafenib treatment is safe and could facilitate anti-tumor immune responses by increasing the infiltration and activation of CD8+ T-lymphocytes inside the tumor. The triple combination treatment inhibited both growth of the primary tumor and the formation of lung metastases in orthotopic murine HCCs and regressed established tumors in a genetically engineered mouse model of HCC in mice with underlying liver cirrhosis. Although clinical translation of a triple therapy including sorafenib and two immune modulating agents seems challenging, our data highlight the clinical relevance of studying the role of the immune microenvironment in resistance to anti-angiogenic treatment as well as for the future development of immunotherapy in HCC.

Immune checkpoint inhibition is a very promising approach across various tumor types, with multiple clinical trials ongoing, including a trial in HCC (18). A challenging aspect for the development of immunotherapies will be their integration in existing therapeutic regimens (18). Thus, our study may have important implications for the development of immunotherapy in HCC. In line with previous reports, we show that intratumoral CD8+ T-lymphocyte infiltration is limited in human HCC. Moreover, we show that the anti-vascular effects of sorafenib promote hypoxia-mediated immunosuppression, including increased PD-L1 expression in HCC. We also demonstrate that to enhance immunotherapy efficacy in

Author Manuscript Author Manuscript Author Manuscript Author Manuscript

HCC, approaches such as CXCR4 inhibition might be critical to prevent immunosuppression. Alternatively, dose-titration of sorafenib or more selective anti-VEGF/VEGFR2 agents (such as antibodies) might help to inhibit angiogenesis without a pronounced increase in hypoxia and thus synergize with novel immunotherapies against HCC.

In summary, in addition to promoting tumor desmoplasia (13), the SDF1α/CXCR4 pathway also mediates stroma polarization towards an immunosuppressive microenvironment and contributes to systemic disease progression after antiangiogenic treatment in HCC (Fig. 7). Blockade of both CXCR4 and PD-1 prevents suppression of immune cell function in HCC tumors, enhances immune cell tumor penetration and activation, and ultimately delays HCC progression. Further understanding of the complex interaction between antiangiogenic, anti-metastatic and immunotherapeutic agents is warranted to facilitate progress in the systemic treatment of advanced HCC.

Supplementary Material

Refer to Web version on PubMed Central for supplementary material.

Acknowledgments

Financial Support: This study was supported by the National Institutes of Health grants P01-CA080124, R01-CA159258, R21-CA139168, R01-CA126642 and National Cancer Institute/Proton Beam Federal Share Program awards (to D.G.D. and R.K.J.), by the American Cancer Society grant 120733-RSG-11-073-01-TBG (to D.G.D.), by a Max Kade Fellowship (to T.R.), and a Postdoctoral Fellowship from Astellas Foundation for Research on Metabolic Disorders, Japan (to T.H.).

The authors thank V. Chauhan, I. Chen, G. Lauwers, S. Pillai and T. Vardam for useful discussions, and A. Khachatryan, O. Pulluqi, S.C. Min and C. Smith for their outstanding technical support.

List of Abbreviations

HCC	hepatocellular carcinoma
SDF1α	stromal-derived factor 1 alpha
CXCR4	C-X-C receptor type 4
CCL	chemokine (C-C motif) ligand
CXCL	chemokine (C-X-C motif) ligand
MMP	matrix metalloproteinase
EMT	epithelial to mesenchymal transition
IL	interleukin
IFN	interferon
TNF	tumor necrosis factor
TGF	transforming growth factor
Arg	arginase

Author Manuscript Author Manuscript Author Manuscript Author Manuscript

NOS	nitric oxide synthase
Gr-1	myeloid differentiation antigen
Gluc	Gaussia luciferase
PD-1	programmed death receptor 1
PD-L1	programmed death-ligand 1 (CD274)
TKI	tyrosine kinase inhibitor
VEGFR	vascular endothelial growth factor receptor
PDGFR	platelet-derived growth factor receptor
IF	immunofluorescence
PBS	phosphate buffered solution
TIL	T infiltrating lymphocyte
TAM	tumor-associated macrophage
MVD	microvascular density
IHC	immunohistochemistry
Tregs	T regulatory cells
Mst	mammalian sterile 20-like 1

References

1. Cheng AL, Kang YK, Chen Z, Tsao CJ, Qin S, Kim JS, Luo R, et al. Efficacy and safety of sorafenib in patients in the Asia-Pacific region with advanced hepatocellular carcinoma: a phase III randomised, double-blind, placebo-controlled trial. Lancet Oncol. 2009; 10:25–34. [PubMed: 19095497]
2. Llovet JM, Ricci S, Mazzaferro V, Hilgard P, Gane E, Blanc JF, de Oliveira AC, et al. Sorafenib in advanced hepatocellular carcinoma. N Engl J Med. 2008; 359:378–390. [PubMed: 18650514]
3. Carmeliet P, Jain RK. Molecular mechanisms and clinical applications of angiogenesis. Nature. 2011; 473:298–307. [PubMed: 21593862]
4. Jain RK. Antiangiogenesis strategies revisited: From starving tumors to alleviating hypoxia. Cancer Cell. 2014; 26 ePub on November 10, 2014. 10.1016/j.ccell.2014.10.006
5. Semenza GL. Hypoxia-inducible factors in physiology and medicine. Cell. 2012; 148:399–408. [PubMed: 22304911]
6. Wilson WR, Hay MP. Targeting hypoxia in cancer therapy. Nat Rev Cancer. 2011; 11:393–410. [PubMed: 21606941]
7. Huang Y, Goel S, Duda DG, Fukumura D, Jain RK. Vascular normalization as an emerging strategy to enhance cancer immunotherapy. Cancer Res. 2013; 73:2943–2948. [PubMed: 23440426]
8. Huang Y, Snuderl M, Jain RK. Polarization of tumor-associated macrophages: a novel strategy for vascular normalization and antitumor immunity. Cancer Cell. 2011; 19:1–2. [PubMed: 21251607]
9. Motz GT, Coukos G. Deciphering and Reversing Tumor Immune Suppression. Immunity. 2013; 39:61–73. [PubMed: 23890064]
10. Flecken T, Schmidt N, Hild S, Gostick E, Drognitz O, Zeiser R, Schemmer P, et al. Immunodominance and functional alterations of tumor-associated antigen-specific CD8+ T-cell responses in hepatocellular carcinoma. Hepatology. 2014; 59:1415–1426. [PubMed: 24002931]

Author Manuscript Author Manuscript Author Manuscript Author Manuscript

11. Motz GT, Coukos G. The parallel lives of angiogenesis and immunosuppression: cancer and other tales. Nat Rev Immunol. 2011; 11:702–711. [PubMed: 21941296]
12. Huang Y, Yuan J, Righi E, Kamoun WS, Ancukiewicz M, Nezivar J, Santosuosso M, et al. Vascular normalizing doses of antiangiogenic treatment reprogram the immunosuppressive tumor microenvironment and enhance immunotherapy. Proc Natl Acad Sci U S A. 2012; 109:17561–17566. [PubMed: 23045683]
13. Chen Y, Huang Y, Reiberger T, Duyverman AM, Huang P, Samuel R, Hiddingh L, et al. Differential effects of sorafenib on liver versus tumor fibrosis mediated by stromal-derived factor 1 alpha/C-X-C receptor type 4 axis and myeloid differentiation antigen-positive myeloid cell infiltration in mice. Hepatology. 2014; 59:1435–1447. [PubMed: 24242874]
14. Shirabe K, Matsumata T, Maeda T, Sadanaga N, Kuwano H, Sugimachi K. A long-term surviving patient with hepatocellular carcinoma including lymphocytes infiltration--a clinicopathological study. Hepatogastroenterology. 1995; 42:996–1001. [PubMed: 8847059]
15. Eun S, Jeon YK, Jang JJ. Hepatocellular carcinoma with immature T-cell (T-lymphoblastic) proliferation. J Korean Med Sci. 2010; 25:309–312. [PubMed: 20119589]
16. Wada Y, Nakashima O, Kutami R, Yamamoto O, Kojiro M. Clinicopathological study on hepatocellular carcinoma with lymphocytic infiltration. Hepatology. 1998; 27:407–414. [PubMed: 9462638]
17. Fu J, Zhang Z, Zhou L, Qi Z, Xing S, Lv J, Shi J, et al. Impairment of CD4+ cytotoxic T cells predicts poor survival and high recurrence rates in patients with hepatocellular carcinoma. Hepatology. 2013; 58:139–149. [PubMed: 22961630]
18. Hato T, Goyal L, Greten TF, Duda DG, Zhu AX. Immune checkpoint blockade in hepatocellular carcinoma: Current progress and future directions. Hepatology. 2014
19. Yang P, Markowitz GJ, Wang X-F. The hepatitis B virus-associated tumor microenvironment in hepatocellular carcinoma. Natl Sci Rev. 2014; 1:396–412. [PubMed: 25741453]
20. Topalian SL, Hodi FS, Brahmer JR, Gettinger SN, Smith DC, McDermott DF, Powderly JD, et al. Safety, activity, and immune correlates of anti-PD-1 antibody in cancer. N Engl J Med. 2012; 366:2443–2454. [PubMed: 22658127]
21. Barsoum IB, Smallwood CA, Siemens DR, Graham CH. A Mechanism of Hypoxia-Mediated Escape from Adaptive Immunity in Cancer Cells. Cancer Research. 2014; 74:665–674. [PubMed: 24336068]
22. Noman MZ, Desantis G, Janji B, Hasmim M, Karray S, Dessen P, Bronte V, et al. PD-L1 is a novel direct target of HIF-1alpha, and its blockade under hypoxia enhanced MDSC-mediated T cell activation. J Exp Med. 2014; 211:781–790. [PubMed: 24778419]
23. Zhou D, Conrad C, Xia F, Park JS, Payer B, Yin Y, Lauwers GY, et al. Mst1 and Mst2 maintain hepatocyte quiescence and suppress hepatocellular carcinoma development through inactivation of the Yap1 oncogene. Cancer Cell. 2009; 16:425–438. [PubMed: 19878874]
24. Tseng D, Vasquez-Medrano DA, Brown JM. Targeting SDF-1/CXCR4 to inhibit tumour vasculature for treatment of glioblastomas. Br J Cancer. 2011; 104:1805–1809. [PubMed: 21587260]
25. D'Alterio C, Barbieri A, Portella L, Palma G, Polimeno M, Riccio A, Ierano C, et al. Inhibition of stromal CXCR4 impairs development of lung metastases. Cancer Immunol Immunother. 2012; 61:1713–1720. [PubMed: 22399057]
26. Chantrain CF, Feron O, Marbaix E, DeClerck YA. Bone marrow microenvironment and tumor progression. Cancer Microenviron. 2008; 1:23–35. [PubMed: 19308682]
27. Du R, Lu KV, Petritsch C, Liu P, Ganss R, Passegue E, Song H, et al. HIF1alpha induces the recruitment of bone marrow-derived vascular modulatory cells to regulate tumor angiogenesis and invasion. Cancer Cell. 2008; 13:206–220. [PubMed: 18328425]
28. Grunewald M, Avraham I, Dor Y, Bachar-Lustig E, Itin A, Jung S, Chimenti S, et al. VEGF-induced adult neovascularization: recruitment, retention, and role of accessory cells. Cell. 2006; 124:175–189. [PubMed: 16413490]
29. Rolny C, Mazzone M, Tugues S, Laoui D, Johansson I, Coulon C, Squadrito ML, et al. HRG inhibits tumor growth and metastasis by inducing macrophage polarization and vessel

Author Manuscript Author Manuscript Author Manuscript Author Manuscript

normalization through downregulation of PlGF. Cancer Cell. 2011; 19:31–44. [PubMed: 21215706]

30. Zhu AX, Duda DG, Sahani DV, Jain RK. HCC and angiogenesis: possible targets and future directions. Nat Rev Clin Oncol. 2011; 8:292–301. [PubMed: 21386818]
31. Hernandez-Gea V, Toffanin S, Friedman SL, Llovet JM. Role of the Microenvironment in the Pathogenesis and Treatment of Hepatocellular Carcinoma. Gastroenterology. 2013
32. Duda DG, Kozin SV, Kirkpatrick ND, Xu L, Fukumura D, Jain RK. CXCL12 (SDF1alpha)-CXCR4/CXCR7 pathway inhibition: an emerging sensitizer for anticancer therapies? Clin Cancer Res. 2011; 17:2074–2080. [PubMed: 21349998]
33. Hiratsuka S, Duda DG, Huang Y, Goel S, Sugiyama T, Nagasawa T, Fukumura D, et al. C-X-C receptor type 4 promotes metastasis by activating p38 mitogen-activated protein kinase in myeloid differentiation antigen (Gr-1)-positive cells. Proc Natl Acad Sci U S A. 2011; 108:302–307. [PubMed: 21173223]
34. Hanahan D, Coussens LM. Accessories to the crime: functions of cells recruited to the tumor microenvironment. Cancer Cell. 2012; 21:309–322. [PubMed: 22439926]

Author Manuscript Author Manuscript Author Manuscript Author Manuscript

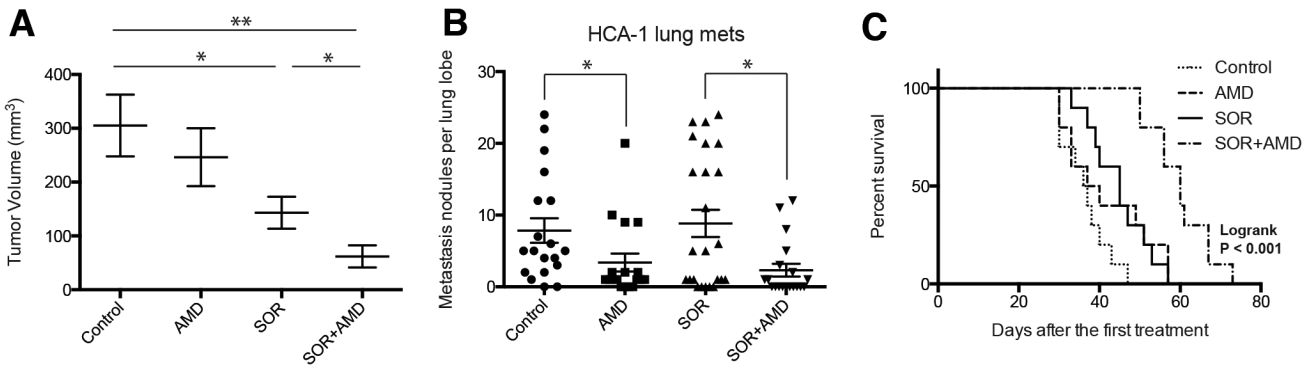

Figure 1. Treatment with the SDF1α/CXCR4 inhibitor AMD3100 plus sorafenib inhibits primary tumor growth, incidence of lung metastasis formation and improves overall survival in orthotopic HCC models

(**A**) While sorafenib (SOR) treatment alone marginally delays HCC growth, the addition of AMD3100 (AMD) to SOR – but not AMD alone – induces an additional significant delay in tumor growth (n=8; *p<0.05, **P<0.01). (**B**) The number of lung metastatic nodules is significantly reduced in AMD-treated mice. (**C**) Overall survival is significantly prolonged only in orthotopic HCC-bearing mice treated with SOR and AMD. Data are representative of at least two independent experiments and are presented as mean±SEM (n=10). *P<0.05; **P<0.01.

Author Manuscript Author Manuscript Author Manuscript Author Manuscript

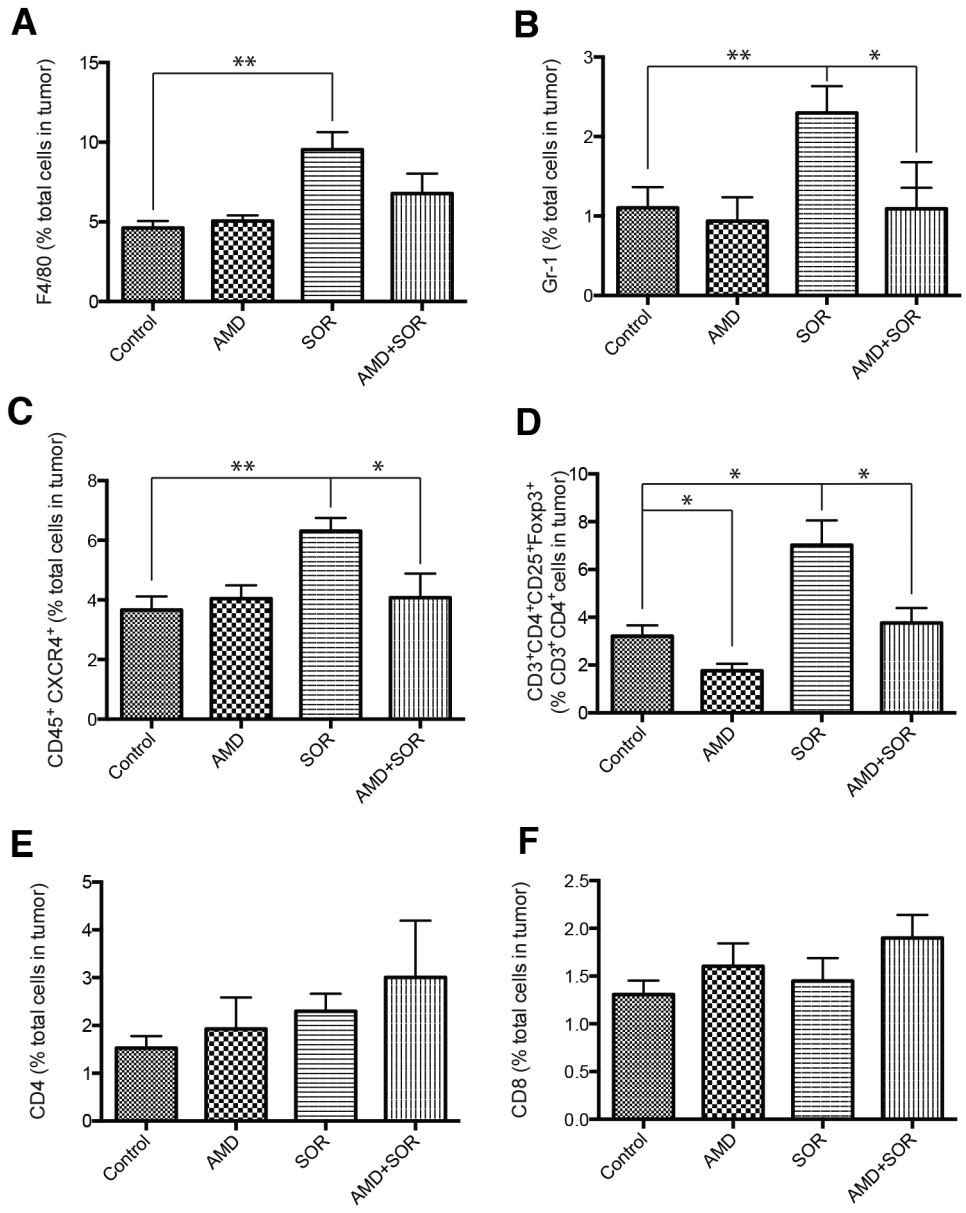

Figure 2. Sorafenib treatment induces a polarization towards a pro-immunosuppressive environment in orthotopic HCA-1 tumors, which is prevented by CXCR4 inhibition in the face of persistent hypoxia

(**A–D**) Changes in viable tumor-infiltrating immune cells in HCA-1 tumors from mice treated with sorafenib with or without AMD3100 versus control analyzed by flow cytometry. The number of 7AAD–CD45+F4/80+ tumor-associated macrophages (**A**), 7AAD–CD11b+Gr1+ monocytes (**B**), 7AAD–CD45+CXCR4+ cells (**C**), and 7AAD–CD4+CD25+FoxP3+ T regulatory (Treg) cells (**D**) significantly increased in sorafenib treated HCCs. Combining AMD3100 treatment with sorafenib prevents these effects. (**E–F**) The number of 7AAD–CD4+CD3+ (**E**) and 7AAD–CD8+CD3+ (**F**) T lymphocytes was not significantly different between the four treatment groups in HCA-1 HCCs. *p<0.05; Data are shown as mean±SEM.

Author Manuscript Author Manuscript Author Manuscript Author Manuscript

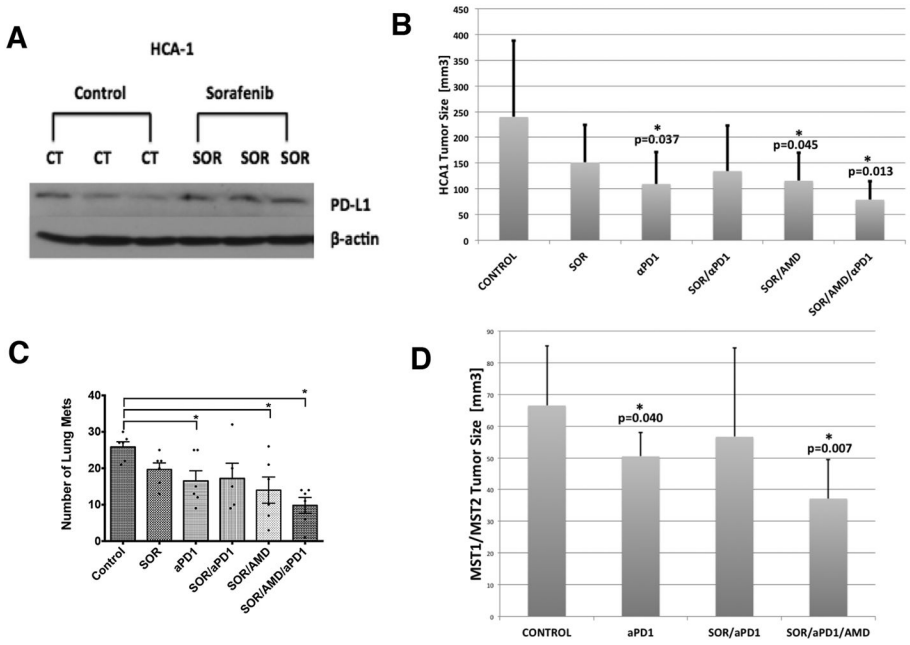

Figure 3. PD-1 blockade is active against HCC in grafted and genetically-engineered models and is facilitated by sorafenib when combined with CXCR4 inhibition

(**A**) Orthotopic HCA-1 tumors were treated when the tumor reached a size of 14mm^3 with sorafenib for 28 days and then the tumors were collected. Western blot analysis shows that PD-L1 expression is increased in HCC tissue after sorafenib treatment compared to control treated tumors. (**B**) PD-1 blockade alone or the combination of sorafenib/AMD3100 significantly delays tumor growth (both $p<0.05$ vs. control). The most effective tumor growth delay is achieved by the triple combination therapy of sorafenib/AMD3100/anti-PD-1 ($p=0.013$ vs. control). (**C**) While the number of lung metastases is significantly reduced by anti-PD-1 treatment or the combination of SOR/AMD3100, the triple therapy of SOR/AMD3100/anti-PD-1 results in most pronounced decrease in lung metastases incidence. (**D**) PD-1 blockade alone ($p=0.04$ vs. control) but not in combination with SOR significantly delays HCC growth in the Mst-mutant mouse model (not significant). The most effective tumor growth delay and regression is achieved by the triple combination therapy of sorafenib/AMD3100/anti-PD-1 ($p=0.007$ vs. control). Data are presented as mean±SEM (N=6 per group). *P<0.05, **P<0.005.

Author Manuscript Author Manuscript Author Manuscript Author Manuscript

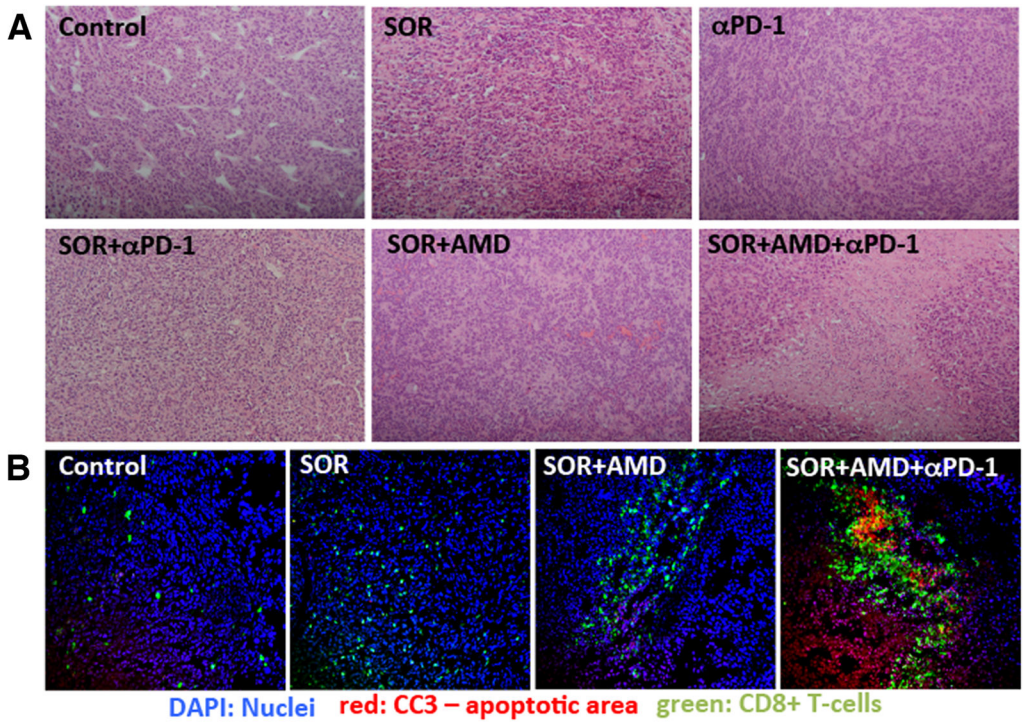

Figure 4. Anti-PD-1 treatment combined with sorafenib and AMD3100 enhances anti-tumor immune responses in HCC

(**A**) Representative H&E staining showing rare areas of necrosis in untreated tumors, and some necrotic areas in sorafenib or anti-PD-1 antibody only treated HCA1 tumors. Sorafenib plus AMD3100 treatment results in further enhancement of tumor necrosis, and triple combination treatment results in extensive necrosis, with lymphocytic immune cell infiltration in the necrotic areas (H&E Staining, 10× magnification). (**B**) Representative immunoflorescence staining for CD8+ T cells (FITC, green) and cleaved caspase-3 (Cy5, red) in frozen HCA1 tumor sections. Counterstaining of nuclei by DAPI (blue). Tumor infiltrating cytotoxic CD8+ cells co-localized with areas of cell apoptosis only in the triple combination treatment group.

Author Manuscript Author Manuscript Author Manuscript Author Manuscript

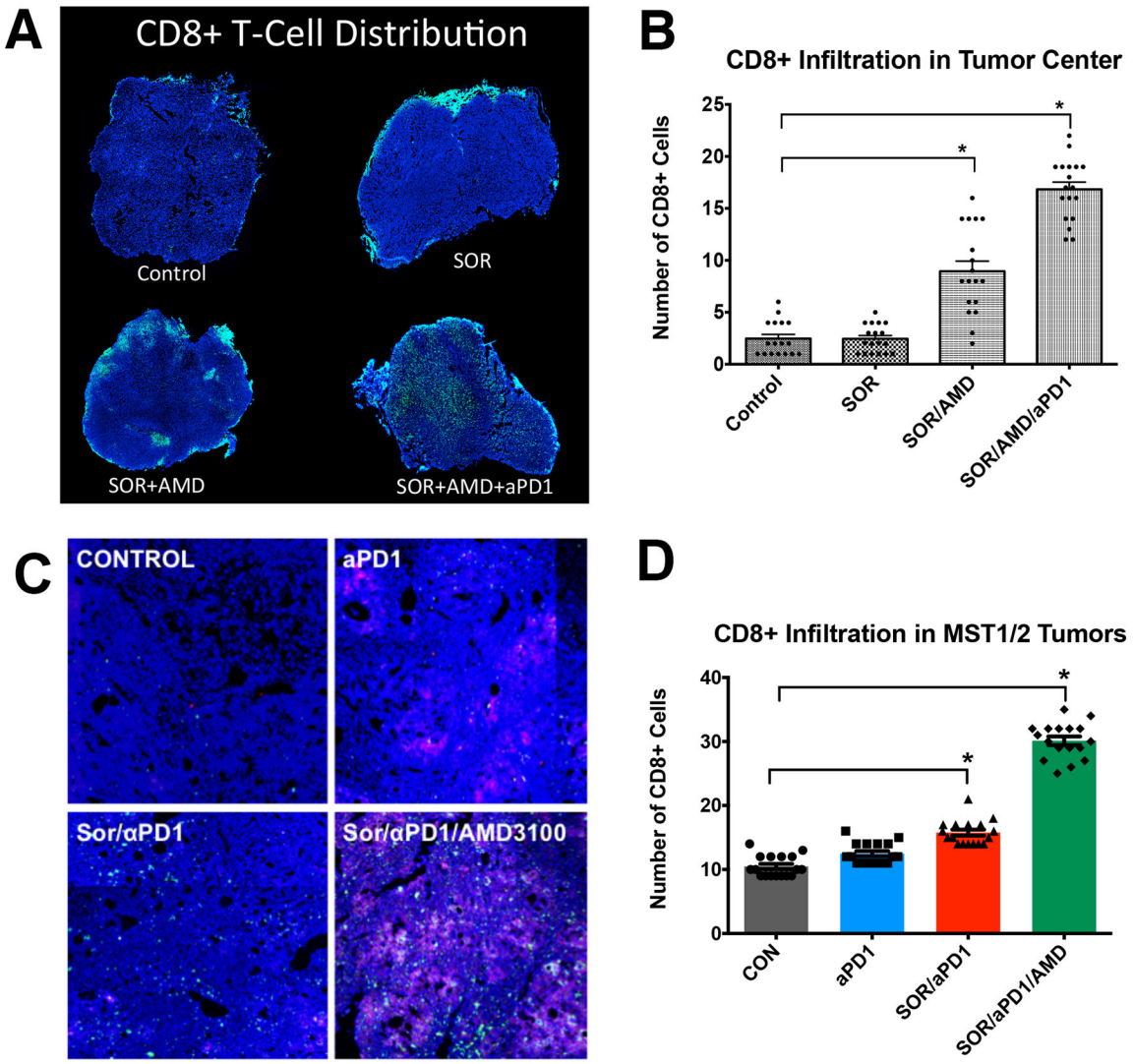

Figure 5. Anti-PD-1 treatment combined with sorafenib and AMD3100 increases intratumoral CD8+ T lymphocyte distribution in HCC

A–D, The number of cytotoxic T lymphocytes infiltrating the tumor proper is increased only in the SOR+AMD3100+αPD1 treatment group. Representative confocal microscopy of immunofluorescence for CD8+ T lymphocytes (FITC, green) in HCC tissue sections (nuclei by DAPI, in blue) from HCA-1 grafted tumors (**A**) and representative regions of HCC tumors in the Mst GEM model. Red areas in the MST tumors indicate apoptotic regions of MST HCC tumors (staining for cleaved-caspase 3, Cy5 in red) (**C**). (**B,D**) Addition of anti-PD-1 antibody changes the distribution of CD8+ T lymphocytes in the tumors: Triple combination treatment results in significantly higher numbers of cytotoxic T lymphocytes in tumor center. Data are mean±SEM (n =5–6 per group) *P<0.05 vs. control.

Author Manuscript Author Manuscript Author Manuscript Author Manuscript

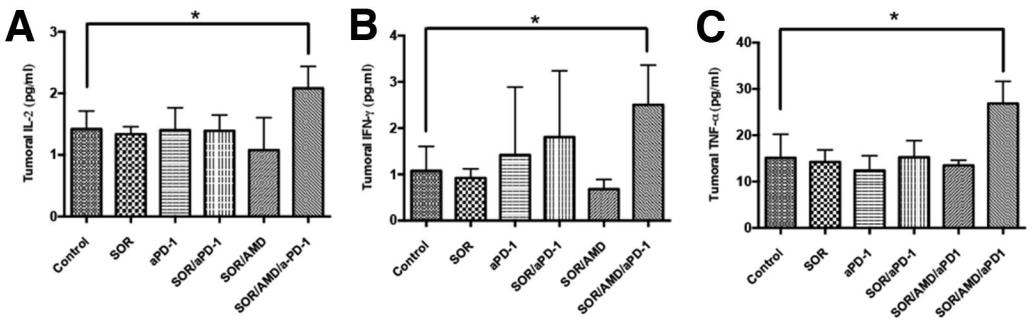

Figure 6. Addition of anti-PD-1 antibody to sorafenib and CXCR4 inhibition increases the expression of biomarkers of T lymphocyte activation in HCC

(**A–C**) PD-1 blockade combined with sorafenib and AMD3100 induces a significant increase of T lymphocyte activation biomarkers IL-2 (**A**), TNF-α (**B**), and IFN-γ (**C**) in HCA-1 tumors versus HCCs in other treatment groups. Data are presented as mean±SEM (N =5 per group) *P<0.05.

Author Manuscript Author Manuscript Author Manuscript Author Manuscript

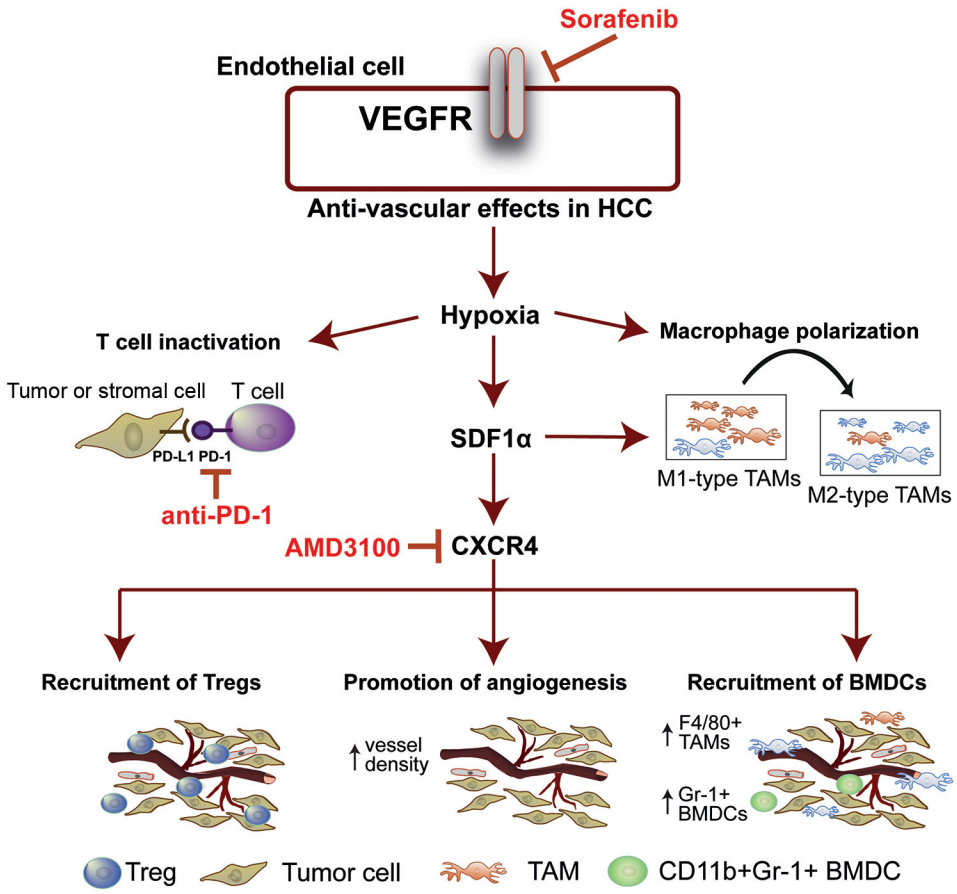

Figure 7.

Sorafenib treatment induces SDF1α/CXCR4 axis-mediated immunosuppression in HCC microenvironment.